Indian Journal of Radio & Space Physics
Vol 40, December 2011, pp 301-310

Monitoring tropospheric radio refractivity over Nigeria Using CM-SAF data derived from NOAA-15, 16 and 18 Satellites

Babatunde Adeyemi[$,*] & Israel Emmanuel

Department of Physics, Federal University of Technology, PMB 704, Akure, Ondo State, Nigeria

[$]E-mail: tundebx@yahoo.com

Received 25 April 2011; revised 23 September 2011; accepted 11 October 2011

The variability and structure of tropospheric refractivity (N) over Nigeria has been studied using monthly data of pressure, temperature and relative humidity for the period 2004-2006 for twenty six stations, obtained from the archives of the Department of Satellite Applications Facility on Climate Monitoring (CM-SAF) DWD, Germany. The data was retrieved from ATOVS observations onboard polar orbiting NOAA-15, 16 and 18 satellites. The results have shown that variations in each region and at different atmospheric levels are influenced by the North–South movement of inter–tropical discontinuity (ITD). Using the analysis of variance (ANOVA) technique on the climatological data, an empirical relationship of the form $N = \omega + \gamma N_s$ (ω, γ constants) have been established between columnar refractivity and its surface value, $N_{s,}$ for the four regions (coastal, Guinea Savannah, midland and sub-Sahelian) in Nigeria. The initial tests carried out on the model using data obtained over the regions for the year 2007 yielded an encouraging result as have been established by the use of Kolmogorov-Smirnov tests.

Keywords: Inter-tropical discontinuity (ITD), Columnar refractivity, Tropospheric refractivity; Surface refractivity, Analysis of variance (ANOVA)

PACS No.: *92.60.hf*

1 Introduction

A reliable operation of ground-based communication systems for various purposes largely depends on the physical state of the atmospheric boundary layer. Meteorological situations of the troposphere in radio paths are governed by various properties of the under surface layer, its physical and geographical as well as climatic features of the region. Changes in atmospheric conditions and its consequent effects on tropospheric radio wave propagation are manifested in the variations of the radio field strengths and the distance to the radio horizons[1-3]. Microwave propagation through the troposphere is affected by varieties of natural phenomena caused by the presence of some meteorological parameters[4-7]. These meteorological parameters, viz. pressure, temperature, and relative humidity have serious effect on radio wave propagation at UHF and microwave frequencies. These effects are analyzed from the study of radio refractive index derived from these meteorological parameters[8]. Since these meteorological parameters vary considerably diurnally and seasonally in the tropics, quantitative knowledge of the refractivity variations is very essential so as to be able to design reliable and efficient radio communication (terrestrial and satellite) systems.

The refractive index in the troposphere falls slowly with height and the resulting refraction causes the radio horizon to appear to be 1.33 times further away than the geometric horizon[9]. Korak[10] in his study on "neutral atmospheric refraction on microwave propagation and its implication on GPS based ranging systems" pointed out that the tropospheric refraction affects microwave propagation by retarding and bending it, causing an error in microwave ranging. Adediji & Ajewole[11], in their study on vertical profile of radio refractivity gradient in Akure, Nigeria, noted that one reason for multipath of electromagnetic wave is bending due to variation in the refractive index distribution along layers of the atmosphere.

The atmospheric refractive index is slightly greater than unity (about 1.0003), hence the refractive index of air is measured by a quantity called the radio refractivity, N, defined as[12,13]:

$$n = 1 + N \times 10^{-6} \quad \ldots(1)$$

$$N = (n-1) \times 10^{6} \quad \ldots(2)$$

Studies by Adeyemi & Adedayo[14] on atmospheric radio refractivity and water vapour density at Oshodi and Kano, Nigeria, revealed that atmospheric radio refractivity is generally high during the rainy season at all the levels of the atmosphere considered while its values fall during the Harmattan period. Bean & Thayers[15] noted that correlation exists between the monthly means of surface refractivity, N_s, and monthly means of the refractivity decrease in the first kilometre above the sea level. Bayong & Djakawinata[16], while trying to study the influence of meteorological factors on tropospheric refractive index over Indonesia using radiosonde data, noted that the value of the index of refraction 'n' near the surface in the maritime continent of Indonesia is about 1.000378 (N=378) in the rainy season of January while the value of the refractive index is about 1.000368 (N=368) in the transition period of October. They concluded that the difference observed in the refractive index values is caused by the difference in the water vapour content in the atmosphere in both the seasons.

Stergios *et al.*[17] observed that from the refractivity variations of the Helenic troposphere, radio refractivity increases from January to June where it appears to reach its peak, and decreases from July to its minimum in August.

Fairall[18], in his study on a top down and bottom-up diffusion model of C_T^2 and C_Q^2 in the entraining convective boundary layer, revealed that within the atmospheric boundary layer (ABL), the atmospheric refractive index fluctuates chaotically in time and in all three spatial directions and near the top of the convective boundary layer, the values of the structure function parameters (which include temperature, water vapour and relative humidity) typically depart from those of the mixed layer forms and increase sharply to high values before decreasing again at greater heights.

The objective of this paper is to study the space – time distribution of tropospheric radio refractivity over Nigeria using data retrieved from NOAA-15, 16 and 18 satellites and to propose an empirical model relating surface radio refractivity, N_S, to radio refractivity aloft for four different regions in Nigeria.

2 Source of data and Processing techniques

The source of upper air climatological data used for present analyses is the Department of Satellite Application Facility on Climate Monitoring (CM-SAF), DWD, Germany. The CM-SAF focuses on the atmospheric part of the essential climatic variables defined within the framework of the Global Climate Observing System (GCOS). The CM-SAF operationally applies the international ATOVS processing package (IAPP) to retrieve humidity and temperature from ATOVS observations onboard NOAA-15, 16 and 18. The ATOVS flies on NOAA polar orbiting satellites, and is composed of Advanced Microwave Sounding Unit (AMSU) and High Resolution Infrared Radiation Sounder (HIRS/3) (HIRS/4 on NOAA-18 and MetOp). The AMSU platform is composed of two separate radiometers, namely AMSU-A and AMSU-B (MHS on NOAA-18 and MetOp). AMSU-A and –B are cross-track scanning total power radiometers with instantaneous fields of view (FOV) of 3.3° and 1.1° providing nominal spatial resolutions at nadir of 48 km and 16 km, respectively. The 15 AMSU-A channels primarily provide temperature sounding of the atmosphere through channels located in the 57 GHz O_2 absorption band. It also has three channels (23.8, 31.4, 89 GHz) that provide information on tropospheric water vapour, precipitation over ocean, sea ice coverage, and other surface characteristics. AMSU-B has five channels that mainly measure water vapour and precipitation over land and sea. Its frequencies at 183.31±1.00, 183.31±3.00 and 183.31±7.00 GHz are positioned within a water vapour absorption band, and the 89.0 and 150 GHz channels are placed within atmospheric windows. The International ATOVS Processing Package (IAPP) ver 7 is used to retrieve profiles of atmospheric temperature and mixing ratio as well as other different atmospheric parameters at global scales. The validation of water vapour and temperature products is carried out using global radiosonde observations that meet the quality standards of GCOS Upper Air Network (GUAN). The ATOVS retrieved temperature and mixing ratio profiles have been found not to be independent from model fields from the numerical weather prediction model taking into consideration the biases and the bias corrected root mean square error (RMSE). The profiles are vertically integrated and averaged to provide temperature and humidity for 5 layers (925, 775, 600, 400 and 250 mb). The data

obtained for the period 2004-2006 was used in computations of tropospheric refractivity for twenty six stations in Nigeria (Fig. 1), classified into four regions based on their climatic conditions[19]. As in Adeyemi[13], Aro[20] and Adedokun[21,22], radio refractivity between surface and 925 mb level has been labelled as low-level refractivity (N_L); between 775 mbar and 600 mbar as mid-level refractivity (N_m); and between 400 mbar and 250 mbar as upper-level refractivity (N_u).

2.1 Data analysis techniques

The radio refractivity, N, of air for frequencies up to 100 GHz is generally expressed as[8,13]:

$$\mathrm{N} = \frac{77.6}{\mathrm{T}}\left(\mathrm{P} + \frac{4810\ \mathrm{e}}{\mathrm{T}}\right) \qquad \ldots(3)$$

$$N = 77.6\frac{P}{T} + 3.75\times10^5\,\frac{e}{T^2} \qquad \ldots(4)$$

N_{dry} and N_{wet} term components from Eq. (4) are defined as:

$$N_{dry} = 77.6\frac{P}{T};\ N_{wet} = 3.75\times10^5\,\frac{e}{T^2} \qquad \ldots(5)$$

where, P, is the atmospheric pressure in hPa; T, air temperature in Kelvin; and e, water vapour pressure in hPa.

Fig. 1 — Map of Nigeria showing study locations

Meteorological factors (pressure, P; air temperature, T; and relative humidity, H) are obtained directly from the retrieved data. Water vapour pressure, e, on the other hand, was determined using[23]

$$e = \frac{He_S}{100} \qquad \ldots(6)$$

where, H, is relative humidity (%); e_s, saturation vapour pressure (hPa). It should be noted that N_{wet} is mainly responsible for the variability in N within the troposphere[24,25]. N_{wet} contributes about 34% to the total value of N_s while N_{dry} contributes about 66%. Radio refractivity was determined using Eq. (4) for the five different layers.

Then for each region, correlations of (N_S and N_L), (N_S and N_m) and (N_S and N_u) were obtained. High correlation values were found to be predominant at most of the regions, most especially, at the lower and middle levels of the atmosphere (Table 1), therefore, using analysis of variance (ANOVA) technique (table not shown), a linear regression relation of the form

$$N = \omega + \gamma N_S \qquad \ldots(7)$$

was developed taking into consideration the associated F-ratios and the probability values.

3 Result and Discussion

3.1 Space – time distribution of tropospheric radio refractivity

In the coastal region, Figs 2(a-d), both the surface refractivity, N_S, and low-level refractivity, N_L, display double peaks with a dip in between them around July/August. Their mean values during the dry season are 373.3±2.96 and 327.2±2.57, respectively, while during the rainy season they were 374.7±1.37 and 328.4±1.19, respectively. The mid-level refractivity, N_m, on the other hand displays seemingly double peaks with the first in May/June and the other in September. The observed double peaks here are not as conspicuous as in N_L. N_m values are generally lower than those of N_L. This is expected to be so as water vapour decreases with increasing height from the surface. Its average value during the dry season is 217.5±0.95 while during the rainy season, it is 222.9±0.26. Upper level refractivity, N_u, has its values slightly increasing from January to July, after which, it then decreases for the rest of the year. It lies between 109.4±0.085 and 110.3±0.095, with its mean value being 109.8±0.09.

Table 1 — Values of the best fit parameters ω and γ in the regression equation of N_L on N_S, N_m on N_S and N_u on N_S

(a) Low level	k				$N_L + \omega + \gamma N_s$				
Region		Ω	Error in ω	Γ	Error in γ	r	CD, %	F-ratio	p-value
Coastal	12	3.285	0.005	0.868	1.22E-05	0.99	98.0	5.05E+09	0.000
Guinea Savanna	12	3.231	0.012	0.868	3.27E-05	0.99	98.0	7.05E+08	0.000
Midland	12	89.02	0.409	0.688	0.001	0.99	98.0	3.02E+05	0.000
Sub - Sahelian	12	95.73	0.606	0.691	0.002	0.99	98.0	1.17E+05	0.000
(b) Mid level	k				$N_m + \omega + \gamma N_s$				
Region		Ω	Error in ω	Γ	Error in γ	r	CD, %	F-ratio	p-value
Coastal	12	173.7	82.16	0.126	0.219	0.18	31.9	0.329	0.060
Guinea Savanna	12	77.21	31.46	0.383	0.084	0.82	67.5	20.76	0.034
Midland	12	149.8	4.874	0.209	0.015	0.96	95.2	196.3	0.000
Sub - Sahelian	12	161.7	3.702	0.173	0.012	0.98	95.2	196.9	0.000
(c) Upper level	k				$N_u + \omega + \gamma N_s$				
Region		Ω	Error in ω	Γ	Error in γ	r	CD, %	F-ratio	p-value
Coastal	12	124.8	7.875	-0.040	0.021	-0.52	26.7	3.643	0.000
Guinea Savanna	12	109.5	3.166	0.001	0.009	0.03	0.00	20.76	0.034
Midland	12	108.5	0.722	0.004	0.002	0.50	24.7	3.286	0.000
Sub - Sahelian	12	109.6	0.405	0.001	0.001	0.17	2.91	196.9	0.000

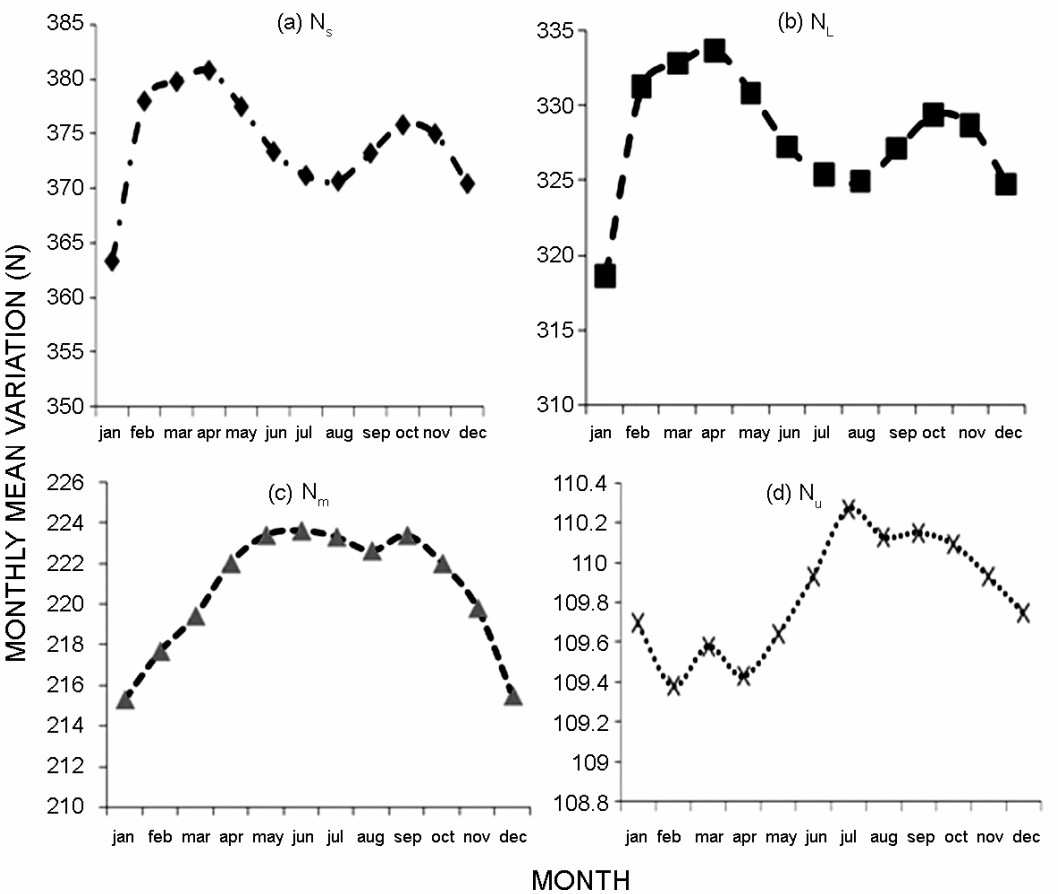

Fig. 2 — Monthly mean variations of: (a) surface refractivity, N_s; (b) low level refractivity, N_L; (c) mid level refractivity, N_m; (d) upper level refractivity, N_u in the coastal region

In the Guinea Savannah region, average N_S and average low-level refractivity display similar pattern with those of the coastal region [Figs 3(a-d)]. Here double peaks with a dip in between them in June-August are also discernible. The June-August dip is characterized by a slight increase in July. Their mean values during the dry season are 370.4±4.48 and 324.7±3.89, respectively. During the rainy season, they are 376.2±3.32 and 329.7±2.88, respectively. $N_{m,}$ on the other hand, display double peaks with a dip in between them lasting between June and August. This depression is more conspicuous than in N_m for coastal region. Its mean value is 219.7±1.09. Upper-level refractivity, N_u, produces a single peak in June. The values are uniformly low, and lie between 109.4± 0.05 and 110.2± 0.06 throughout the year. They gave a mean value of 109.9± 0.065

In the midland region, the structure of N_S and N_L are well related to those of the Guinea savannah region [Figs 4(a-d)]. They are comparably low during the dry months (November – March), with mean values of 294.5±5.19 and 291.5±3.64, respectively. During the rainy months (April – October), high values of N_S and N_L are discernible. Their mean values are 349.5±3.26 and 329.3±2.20, respectively. N_m displays a single peak during May and August with low values prevailing during the dry season and high values characterizing the rainy season. Mean N_m values during the dry and rainy periods are 211.0±0.65 and 222.4±1.13, respectively. In the case of N_u, its values gradually decrease from January to April. The month of April seems to be where the minimum for N_u occurs. A gently increasing trend was then noticeable between April and July. July is the month where the annual peak occurred. Its mean value is 109.819 ± 0.0642 and its range lies between 109.4±0.0643 and 110.2±0.0641 showing that in both the coastal and guinea savannah regions, N_u is uniformly low.

In the sub-Sahelian region, the variations observed in the refractivity parameters are almost similar to those of the midland region [Fig 5(a-d)]. N_S and N_L

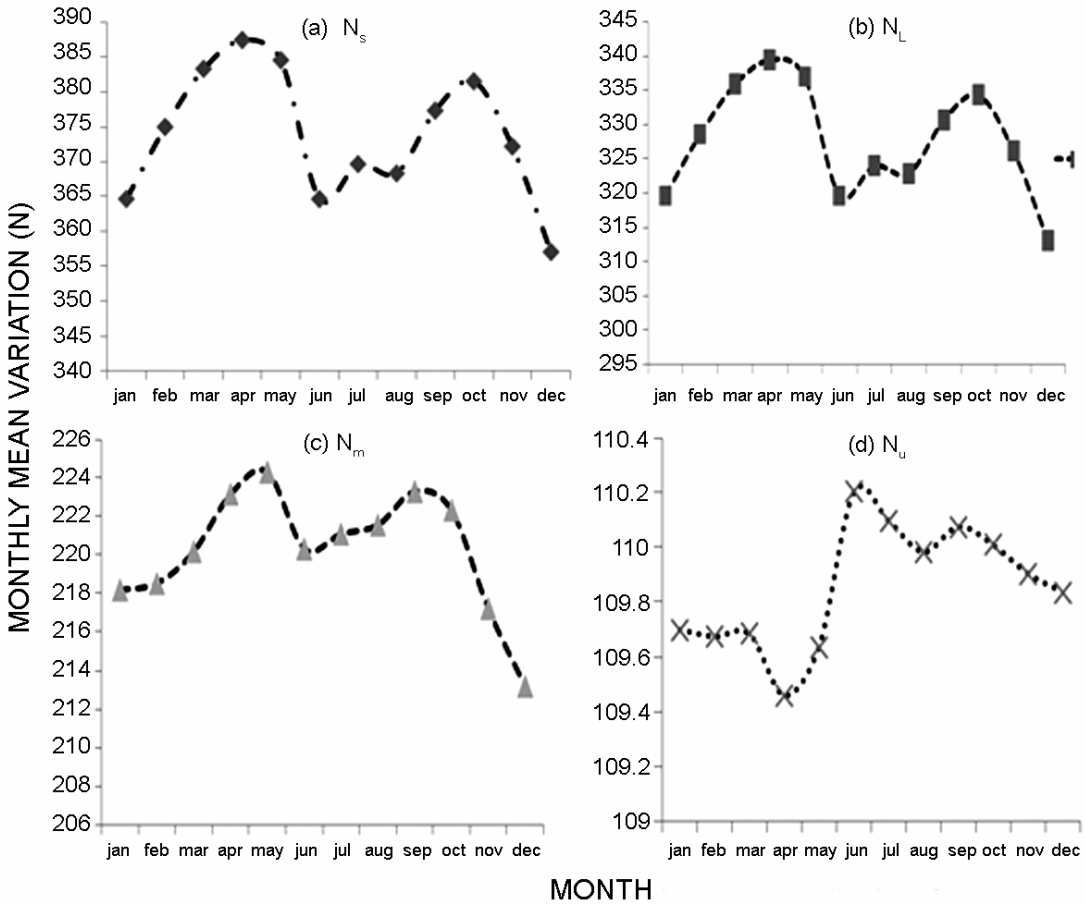

Fig. 3 — Monthly mean variations of: (a) surface refractivity, N_s; (b) low level refractivity, N_L; (c) mid level refractivity, N_m; (d) upper level refractivity, N_u at Guinea Savanna region

are low during the dry months with mean refractivities of 251.7±3.47 and 269.4±2.52, respectively. Their values are high during the rainy season with mean refractivities of 327.2±11.57 and 321.9±7.90, respectively. The variations observed in N_m over this region resemble those of N_S and N_L. But the mean refractivity values of N_m are lower than those of N_S and N_L; they are 205.2±1.56 and 218.2±2.29 during the dry and rainy seasons, respectively. N_u, on the other hand, has almost uniform values throughout the year. However, its value gently decreases during the late dry season (January – April) before it rises, gently, to its highest value in December. Its mean value is 109.9 ± 0.064 and it lies between 109.3±0.065 and 110.1±0.063.

From the foregoing, the observed variations in the refractivity parameters are attributable to the prevailing weather conditions pervading the country (ref. 3). The Nigeria troposphere is characterized by two seasons. They are the Harmattan and the rainy season periods. During the Harmattan period, the Nigeria troposphere is characterized by dry dust particles transported from Azores's sub-tropical high pressure system in the Sahara desert by the north-easterly tropical continental (cT) air mass blowing inland. This coincides with the period of no rain. The rainy season, on the other hand, is characterized by high humidity (heavy rainfall) brought about by the south-westerly tropical maritime (mT) air originating from the southern hemisphere. Wedged in between the air masses, is a front known as inter-tropical discontinuity (ITD) (refs 26,27). The ITD migrates in north-south and south-north direction reaching its maximum northward extent 22-25°N in August and its southward extent 4-6°N in January. While migrating, the ITD oscillates backward and forward within a few latitudinal points. In January, all regions north of 4°N are under the influence of the cT air.

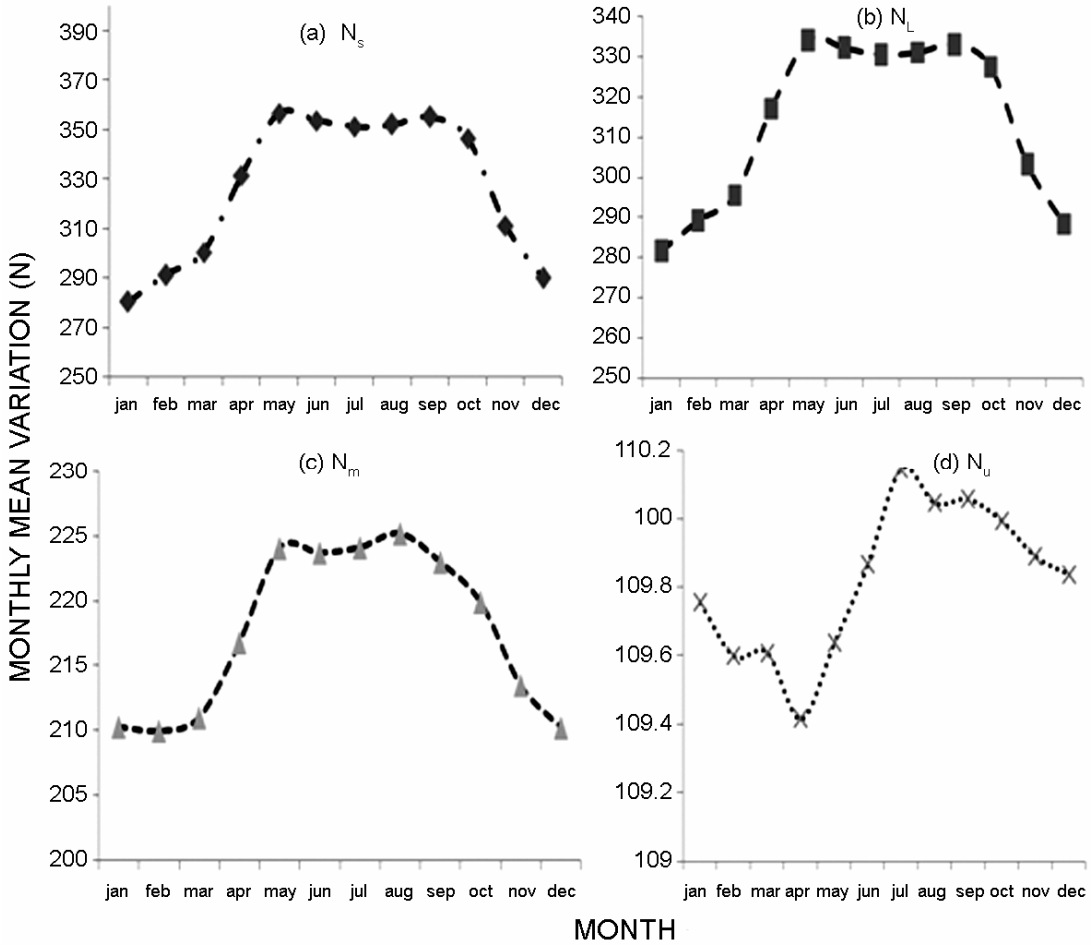

Fig. 4 — Monthly mean variations of: (a) surface refractivity, N_s; (b) low level refractivity, N_L; (c) mid level refractivity, N_m; (d) upper level refractivity, N_u at the midland region

Conditions are such that little or no precipitation is experienced and refractivity parameter values are low, and show marked decrease from the coast inland. During March and April, the ITD position would be between 10°N and 15°N meaning that the regions are now beginning to experience little amount of rainfall making variability in the refractivity parameters to be higher. On reaching its most northern position in August, all areas in Nigeria would have been subjected to widespread rainfall and increased cloud cover. N_m and N_u values increase and become less variable. N_S and N_L on the other hand, in the coastal and guinea savannah regions, experience lower values than they are in the midland and sub-sahelian regions. This is as a result of the existence of the little dry season that often pervades the area around the West-African coast in August.

3.2 Regression analysis

Using Eq. (7), N can be replaced by N_L, N_m, or N_u and the corresponding parameters ω and γ evaluated. The values of the parameters ω and γ for N_L, N_m, and N_u together with the correlation coefficient, r, coefficient of determination, CD and probability (p–value) at which the null hypothesis was either accepted or rejected are as shown in Table 1(a-c). The degree of association evident in Table 1 shows that N_S is better associated with low-level refractivity (N_L) than those of N_m and N_u at all the regions. The degree of association between N_S and N_m has also been found to be higher at both the midland and sub-Sahelian regions than at the coastal and Guinea Savannah regions. Regression relations obtained for all the refractivity parameters are statistically significant at all the levels and at the regions except N_m in the coastal region which is statistically insignificant (p-value = 0.060).

To verify the reliability of the linear relations obtained in Table 1, they were then applied to evaluate refractivity parameters at the different levels and at the regions using satellite data for the year 2007. This was first done annually (January –

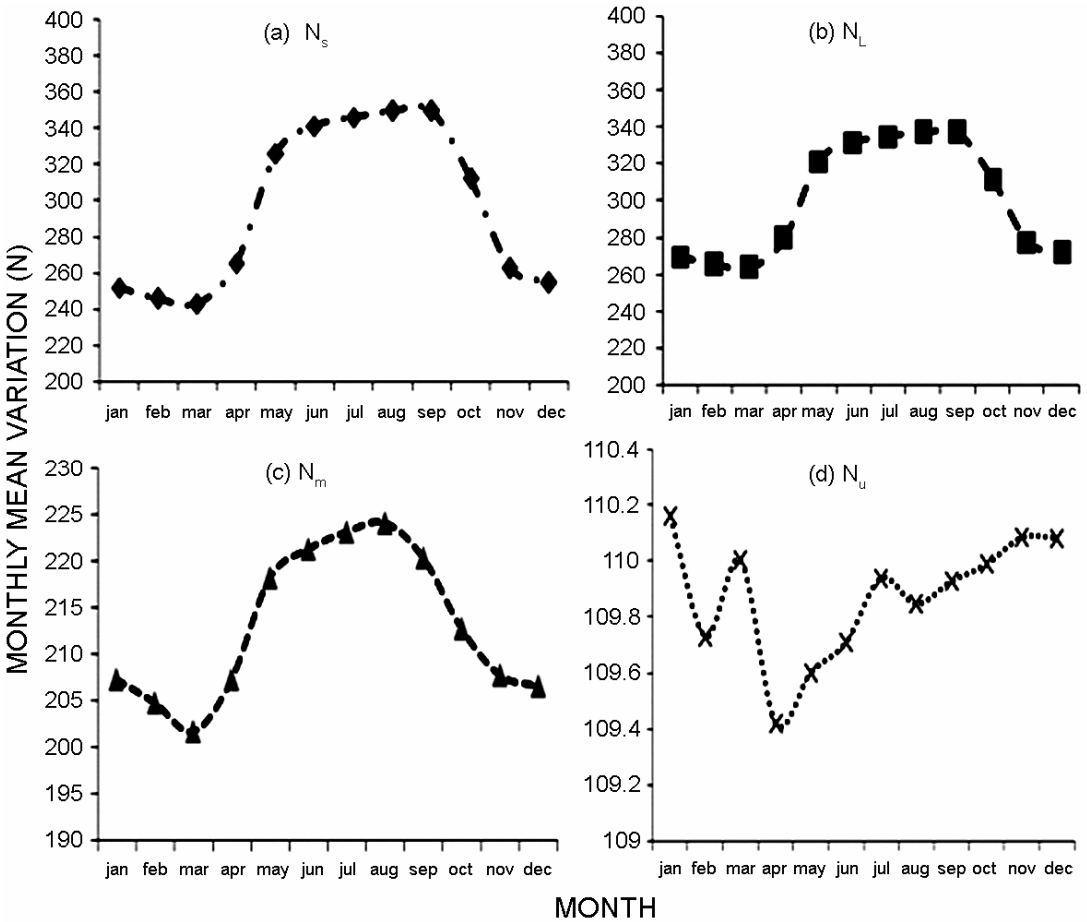

Fig. 5 — Monthly mean variations of: (a) surface refractivity, N_s; (b) low level refractivity, N_L; (c) mid-level refractivity, N_m; (d) upper-level refractivity, N_u at the sub-Sahelian region

December); and then for the different seasons: dry season (November – March); and rainy season (April – October). The results of these, as compared with the actual and calculated values, are shown in Table 2. The agreement between them is remarkable.

3.3 Kolmogorov – Smirnov (KS) test

In order to determine whether any agreement exists between the actual distribution function $F_k(x)$ and each generated series $F_c(x)$, the Kolmogorov-Smirnov (KS) test was applied (refs 13,22,24,28). The KS test is used to determine whether agreement exists between the actual and calculated values. The maximum deviation between $F_k(x)$ and $F_c(x)$ is:

$$D_k = \max \left| F_k(x) - F_c(x) \right| \quad \ldots(8)$$

where, x, is ordered in ascending order such that $0 \leq x_1 \leq x_2 \leq x_3 \leq \ldots\ldots\ldots \leq x_k$.

For k observations,

$$F_k(x) = \frac{Number\ of\ values \leq x}{k}$$

is the actual distribution function. Using observed values, $F_c(x_j)$, j = 1,2,3,……. k, are the values of $F_c(x)$ evaluated at $x_1 \leq x_2 \leq x_3 \leq \ldots.. \leq x_k$. It has been chosen to compare the D_k values with the critical values of D_k for the 5 percent significant level (ref 14,28).

$$D_{k(\alpha=0.05)} = \frac{1.3581}{k^{1/2}} \quad \ldots(9)$$

Hence, if the value of D_k obtained exceeds that of $D_{k(\alpha = 0.05)}$, the two functions are not close enough to be related. This criterion is used to judge the degree of fit or relationship, if any, of the two functions under consideration. On applying this test to the refractivity parameters at different levels and for regions, the results obtained are shown in Tables 3 and 4.

Hence, as shown in Table 3, the actual and model functions are related at all the regions at the lower and upper levels. At the middle level and for coastal and guinea savanna regions, their values showed insignificance. This may be because, as is common to all surface based models, perturbations due to disturbances, which originate (ref. 22) from within the

Table 2 — Application of proposed model for each of the regions annually and seasonally

(a) Coastal region	k	N_s	N_L=3.286+0.868N_s		N_m=173.7+0.126N_s		N_u=124.8-0.040N_s	
			(N-Units)					
			Actual	Calculated	Actual	Calculated	Actual	Calculated
Annually	12	372.6	326.2	326.6	220.1	220.6	110.0	109.9
Dry season	5	369.7	324.1	324.1	215.8	220.3	109.8	110.0
Rainy season	7	374.6	328.4	328.4	223.3	220.9	110.1	109.8
(b) Guinea Savanna region	k	N_s	N_L=3.231+0.868N_s		N_m=77.21+0.382N_s		N_u=109.5+0.001N_s	
			Actual	Calculated	Actual	Calculated	Actual	Calculated
Annually	12	371.8	325.9	325.9	219.6	219.5	109.9	109.8
Dry season	5	382.0	334.8	334.8	221.8	223.4	110.0	109.8
Rainy season	7	364.5	319.6	319.6	218.0	216.7	109.9	109.8
(c) Midland region	k	N_s	N_L=89.02+0.69N_s		N_m=149.8+0.209N_s		N_u=108.5+0.004N_s	
			Actual	Calculated	Actual	Calculated	Actual	Calculated
Annually	12	329.1	315.2	315.3	217.1	218.5	109.9	109.8
Dry season	5	293.7	290.9	290.9	209.8	211.2	109.8	109.7
Rainy season	7	354.3	332.6	332.6	222.3	223.8	109.9	109.9
(d) sub - Sahelian region	k	N_s	N_L=95.73+0.691N_s		N_m=161.7+0.173N_s		N_u=109.6+0.009N_s	
			Actual	Calculated	Actual	Calculated	Actual	Calculated
Annually	12	293.9	298.8	298.8	212.6	212.7	109.9	109.8
Dry season	5	250.2	268.4	268.6	205.3	205.1	110.0	109.8
Rainy season	7	325.2	320.5	320.3	217.9	218.1	109.8	109.8

middle troposphere and whose effects are not quickly communicated to the surface, may not be effectively accounted for by the model. In addition, over the hinterland of West Africa, the ITD surface is known to slope southwards with the moisture-laden south westerlies forming a wedge under a drier north-easterlies[29]. Therefore, a station's position relative to ITD is an important factor determining the structure of the moisture profile over the station. When a shallow moist layer is overlain by a deep dry layer, a model based on surface parameter may overestimate refractivity parameters aloft, and on the other hand, where a dry layer is interspersed by a deep moist layer, an underestimation may result. These limitations may then affect to a greater extent, the effectiveness of the model. The actual and model functions for the mid-level refractivity during the dry and rainy seasons showed the same trend with it being extended to the midland region (Table 4).

4 Conclusions

Using CM-SAF water vapour and temperature products retrieved from Advanced TIROS Operational Vertical Sounder (ATOVS) onboard National Oceanic and Atmospheric Administration (NOAA) satellites NOAA-15, 16, 18, it was possible to establish that seasonal variations of refractivity parameters over Nigeria is dependent upon the north-south movement of the intertropical discontinuity (ITD). This is in consonant with the findings of Balogun[30] and Garbutt *et al.*[31], who have used radiosonde data obtained over Nigeria to investigate precipitation and precipitable water variations and have concluded that differences in precipitation climatologies of the different regions in Nigeria account for the observed differences in the variations of their weather parameters; and that the variations observed in this weather parameters are dependent upon the north-south transect of the ITD. Applying the analysis of variance (ANOVA) technique, a linear relation of the form

$N = \omega + \gamma N_S$ (ω, γ, are constants)

connecting the level refractivity parameters, N-units (low-level refractivity, N_L; mid-level refractivity, N_m; and upper-level refractivity, N_u) with surface refractivity, N_S, have also been established from the satellite data for each region in Nigeria. The difference observed in precipitation climatologies of the different regions has made it impossible to obtain a single model that fits adequately the entire Nigeria region. These relations when used to evaluate refractivity aloft obtained over each of the regions during the year 2007 yielded an encouraging result. On applying the KS test to the evaluated refractivity parameters, the actual and model functions are related at almost all the levels considered at all the regions.

Table 3 — Result of KS test on actual and model results on an annual basis

Region	D_k (α=0.05)	N_L	N_m	N_u
		D_L	D_m	D_u
Coastal	0.392	0.001	0.662*	0.130
Guinea savanna	0.392	0.002	0.643*	0.034
Midland	0.392	0.027	0.325	0.043
Sub - Sahelian	0.392	0.069	0.292	0.048

*Association does not exist between actual and model values at 5 percent significant level

Acknowledgements

The authors wish to express their gratitude to the officials and management of the Department of Climate Monitoring SAF, Deutscher Wetterdienst, Offenbach, Germany for providing the data. The efforts of Dr Jorg Schulz and Mr Markus Jonas of the same Department, in making sure that the data were available in ASCI format during the visit of the corresponding author to CM-SAF is also greatly appreciated.

Table 4 — Result of KS test on actual and model N_L, N_m and N_u values during the dry and the rainy seasons

Region	D_k (α=0.05)	Value of D_k for various refractivity parameters during the dry season			D_k (α=0.05)	Values of D_k for various refractivity parameters during the rainy season		
		D_k for N_L	D_k for N_m	D_k for N_u		D_k for N_L	D_k for N_m	D_k for N_u
Coastal	0.607	0.002	1.589*	0.311	0.513	0.000	0.557*	0.083
Guinea savanna	0.607	0.002	0.809*	0.072	0.513	0.004	1.103*	0.058
Midland	0.604	0.066	0.636*	0.069	0.513	0.034	0.558*	0.073
Sub - Sahelian	0.607	0.165	0.421	0.091	0.513	0.079	0.500	0.082

*Association does not exist between actual and model values at 5 percent significant level

References

1 Kulshresta S M & Chatterjee K, Radio climatology of India: Radio refractive index near the ground surface, *Indian J Meteorol Geophys*, 17 (3) (1965) pp 367-384.

2 Mitra A P, Reddy B M, Radicella S M, Oyinloye J O & Feng S, *Handbook on Radio propagation for tropical and sub-tropical countries* (URSI Committee on developing countries UNESCO subvention, ICTP, Italy), 1987.

3 Willoughby A A, Adimula I A & Sorunke A O, Characteristics of surface radio refractivity over Ilorin, Nigeria, *Nigeria J Phys*, 15 (1) (2003) pp 45-50.

4 Crane R K, Fundamental limitations caused by RF propagation, *Proc IEEE (USA)*, 69 (2) (1981) pp 196-209.

5 Anderson K D, Interference of refractivity profiles by satellites ground RF measurements, *Radio Sci (USA)*, 17 (3) (1982) pp 653-663.

6 Anthony R C, Chris Rocken, Sergey V, Solokors Kij & Kenneth D Anderson, *Vertical profiling of atmospheric refractivity from ground based GPS* (American Geophysical Union, USA), 2002.

7 Adeyemi B, Surface water vapour density and tropospheric radio refractivity linkage over three stations in Nigeria, *J Atmos Sol-Terr Phys (UK)*, 68 (2006) pp 1105-1115.

8 Bean B R & Dutton F J, *Radio meteorology*, National Bureau of Standard monographs 92 (US Department of Commerce, Washington), 1966.

9 Hall M P M, Barclay L W & Hewit M T, *Propagation of radio wave* (IEEE, USA), 1996.

10 Saha Korak, Parameswaran K & Raju C Suresh, Tropospheric delay in microwave propagation for tropical atmosphere based on data from the Indian subcontinent, *J Atmos Sol-Terr Phys (UK)*, 69 (2007) pp 875-905.

11 Adediji A T & Ajewole M D, Vertical profile of radio refractivity gradual in Akure Southwest Nigeria, *Prog Electromagn Res (Hong Kong),* 14 (2008) pp 157-168.

12 Babalola M T, Studies on the vertical model of of the radio refractivity in Nigeria, *Africa J Sci (Nigeria*), 2 (1) (1998) pp 1-10.

13 Adeyemi B, Tropospheric radio refractivity over three radiosonde stations in Nigeria, *Ife J Sci (Nigeria)*, 6 (2) (2004) pp 167-176.

14 Adeyemi B & Adedayo K D, Atmospheric radio refractivity and water vapour density at Oshodi and Kano, Nigeria, *Nigeria J Pure Appl Phys,* 4 (1) (2005) pp 11-12.

15 Bean B R & Thayer G D, Models of the atmospheric refractive index, *Proc Inst Radio Eng (USA),* 47 (5) (1959) pp 740-755.

16 Bayong T H & Djakawinata S, The influenced of meteorological factor, on tropospheric refractive index over Indonesia, *J Mater Sci (USA)*, 4 (1) (1999) pp 1-12.

17 Stergios A I & Thomas D X, Ten years analysis of tropospheric refractivity variations, *Ann Geophys (Germany)*, 47 (4) (2004) pp 1333-1338

18 Fairall C W, A top down and bottom-up diffusion model of C_T^2 and C_Q^2 in the entraining convective boundary layer, *J Atmos Sci (USA)*, 44 (1987) pp 1009-1017.

19 Olaniran O J & Sumner G N, A study of climatic variability in Nigeria based on the onset, retreat, and length of the rainy season, *Int J Climatol (UK)*, 9 (1989) pp 253-269.

20 Aro T O, Analysis of data on surface tropospheric water vapour, *J Atmos Terr Phys (UK)*, 38 (1975) pp 565-571.

21 Adedokun J A, Intra layer/mid tropospheric precipitable water vapour relations and precipitation in West Africa, *Arch Metorol Geophys Bioclimatol B (Austria)*, 33 (1983) pp 117-130.

22 Adedokun J A, On a relationship for estimating precipitable water vapour aloft from surface humidity over West-Africa, *J Clim (USA),* 6 (1986) pp 161-172.

23 International Telecommunication Union-Radiocommunication sector (ITU-R), *The radio refractivity index: its formula and refractivity data, Rec. ITU-R P453* (ITU, Geneva), 1997.

24 Adedokun J A, Surface humidity and precipitable water vapour linkage over west and central Africa: Further clarification and evaluation of existing models, *Int J Clim (UK)*, 9 (1989) pp 425-433.

25 Agunlejika & Raji, Electrical evaluation of water term of refractivity in Nigeria, *Int J Eng Appl Sci (Nigeria*), 2 (2) (2010) pp 63-68.

26 Adedokun J A, West African Precipitation and dominant atmospheric mechanisms, *Arch. Meteorol Geophys Bioclimatol A Meteorol Geophys (Austria),* 27 ((1978) pp 289-310.

27 Adeyemi B & Babalola Y A, Diurnal variations of absolute humidity at Ibadan and Minna, *Nigeria J Sci Eng Technol*, 7 (2) (2000) pp 2371-2375.

28 Kendall M & Stuart A, *The advanced theory of statistics Vol 2*, 4th edition (Charles Griffin, London), 1979, pp 476.

29 Leroux M, La dynamique des Precipitations en Afrique occidental Asecna 39 Dakar Senegal, *J Clim (USA)*, 6 (1971) pp 161-172.

30 Balogun E E, Seasonal and spatial variations in thunderstorm activity over Nigeria, *Mon Weather Rev (USA)*, 36 (7) (1981) pp 192-197.

31 Garbutt O J, Stern R D, Dnnett M D & Elston J, A comparison of the rainfall climate of eleven places in West Africa using a two-part model for daily rainfall, *Arch Meterol Geophys Bioclimatol B (Austria),* 29 (1981) pp 137-140.